Research of the remaining oil displacement in Chang 8 low permeability reservoir in Fanxue area of Ordos Basin

Research of the remaining oil displacement in Chang 8 low permeability reservoir in Fanxue area of Ordos Basin

Yanglong Wang [1, 2], Qibin Yan [1, *], Jiao Yan [1, 3], Qiang Deng [3, 4]

[1] School of Geoscience and Technology, Southwest Petroleum University, Chengdu 610500, China
[2] Dingbian Oilfield, Yanchang Oilfield Company, Yulin, 718600 China.
[3] Shaanxi Province Key Laboratory of Environmental Pollution Control and Reservoir Protection Technology of Oilfields, Xi'an Shiyou University, Xi'an, 710065 China
[4] State Key Laboratory of Petroleum Pollution Control, CNPC Research Institute of Safety and Environmental Technology, Beijing, 102200 China

*Corresponding author e-mail: yqb2640@sina.com

Abstract. In Fanxue area of Ordos Basin, Chang 8 Oil Group has been in the development stage, the current development of more difficult and costly. In this paper, Chang 8 layers in this area are studied by using reservoir sedimentology, logging geology, petroleum geology, petrophysics, 3D reservoir modeling and numerical simulation and laboratory analysis techniques. The reservoir distribution pattern, remaining oil distribution pattern and well pattern optimization provide relevant technical results for the later development and provide guarantee for increasing reserves and production.

1. Introduction

Compared with conventional reservoirs, the pore structure of low-permeability reservoirs is different, and the pore structure is more complicated, which has a significant impact on reservoir oil and gas communication capacity and productivity [1-3]. At present, the study on the pore structure of low permeability reservoirs is more detailed, not only the pore structure type, pore throat width and connectivity, but also the relationship with reservoir seepage capacity [4-8]. The research on the formation and distribution of remaining oil is a worldwide problem in the world oil and gas industry. It is also the research focus of high-exploration areas at home and abroad, and is one of the core technologies for oil and gas field development. At present, the development process of the world oil and gas fields can only produce 30% of the total oil and gas reserves, while more than half of the oil and gas is still in a difficult state. Most of the oil fields in the central and eastern parts of China are now in the stage of high water cut and high recovery, and the output of crude oil is decreasing [9-12]. The development of residual oil in low-permeability and ultra-low-permeability reservoirs has become a more difficult problem in the domestic petroleum industry, and its development potential is huge. The paper points to the problems of "not injecting, not collecting", more residual reserves, scattered distribution and lower degree of utilization, and the complex geological features of the Chang 8 oil-bearing formation in the Fanxue Oilfield of Dingbian Oilfield [13-15]. The characteristics of strong heterogeneity, poor water injection development and difficult development are studied. The formation

mechanism, storage and spatial distribution of microscopic residual oil are important research contents for oil-bearing and enhanced oil recovery in oilfield evaluation reservoirs. Due to the small size of microscopic residual oil, the influencing factors are complex, and various indoor experiments are needed. Based on the established reservoir classification evaluation system, the selected three types of reservoir core samples were used to study the distribution law of microscopic residual oil.

2. Experimental

2.1. Materials

This experimental device is a real sandstone micro-model displacement experiment system assembled by Northwest University. Sandstone model samples from Changqing Oilfield.

2.2. Microscopic water flooding characteristics experiment

The sandstone model samples used in the experiment are comprehensively analyzed based on the oil test results of the oil layer in the study area, the observation of conventional flakes, and the observation of the cast flakes. When the samples are selected, different reservoirs in the study area are selected according to the reservoir classification criteria established in the previous period. The typical production wells of the type are used to make experimental models in cores with different sand bodies, different perforation sections, and different sedimentary microfacies. The real sandstone microscopic model is made by the above-mentioned actual core after being extracted, dried, sliced and grounded, and then bonded between two pieces of glass. The model has a size of about 2.5cm × 2.5cm, a pressure bearing capacity of 0.2MPa, a temperature resistance of 200°C, and a pressure and temperature resistance of 100°C.

2.3. Microscopic model water flooding experiment

Oil-water interaction is actually a simulation of oil and gas entering the reservoir and water injection development process, so the experimental steps include vacuuming saturated water, oil flooding and water flooding. The experimental simulated oil and simulated water were prepared according to the actual formation crude oil viscosity, the formation water and the nature and composition of the injected water. Firstly, the original oil saturation and the irreducible water saturation are calculated by the area statistical method. The residual oil saturation and residual water saturation are calculated by water flooding to calculate the oil displacement efficiency. Finally, according to the observed experimental phenomena, the analysis and interpretation are carried out.

2.4. Core water flooding NMR experiment

The inverse relationship between reservoir pore size and hydrogen nuclear relaxation rate is the theoretical basis for studying rock pore structure by NMR T2 spectroscopy. The distribution of fluid in the rock sample has a relaxation time limit. Above this limit, the fluid is in a free state, which is a movable fluid; below this limit, the fluid in the pore is bound by capillary force or viscous force, and is in a restrained state for binding fluids. The relaxation time limits of different reservoirs (the cutoff value of the movable fluid T2) are different. These two parameters of the movable fluid combine the information of reservoir storage capacity and fluid occurrence characteristics, and more accurately reflect the characteristics of low permeability sandstone reservoirs.

3. Result and Discussion

3.1. Analyses of microscopic water flooding characteristics

It can be obtained from experiments. There are 8 long reservoir models, the porosity is distributed from 6.32% to 13.72%, and the permeability is distributed at $0.081\times10^{-3}\mu m^2$~ $2.57\times10^{-3}\mu m^2$. The physical properties are generally poor. The model microfacies are mostly in the underwater distributary channel, and only the model microphases of the 4123-1 and 4107-2 wells are in the diversion bay (Table 1).

Table 1. Experimental model parameter statistics

Hashtag	Core number	Reservoir type	Layer	Permeability× $10^{-3}\mu m^2$	Porosity/%	Microphase type
4103-4	7	2		0.17	9.21	Underwater diversion channel
4123-1	2	3		0.081	6.32	Diversion bay
4372-2	1	2		0.23	8.72	Underwater diversion channel
4107-2	5	3		0.092	6.53	Diversion bay
4109-3	9	2	Chang 8	0.28	9.27	Underwater diversion channel
43032-3	3	1		2.57	13.72	Underwater diversion channel
4355-2	2	1		1.47	12.58	Underwater diversion channel
4354	5	2		0.41	8.61	Underwater diversion channel

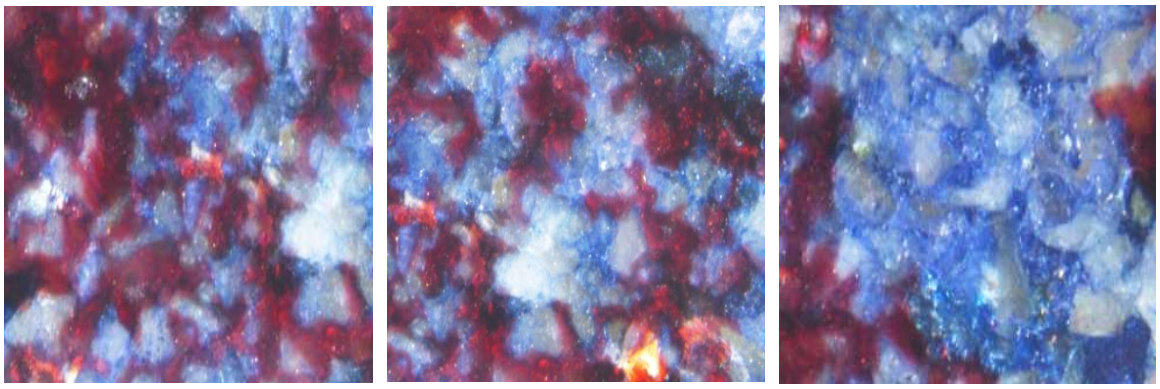

1pv 2pv 3pv

Figure 1. Schematic diagram of real sandstone microdisplacement in Well 4723-2

Different physical properties have different starting pressures, and all models have a rising displacement pressure during water flooding. If you do not continue to increase the displacement pressure, the injected water will not continue to flow. The following describes the microscopic characteristics of different types of reservoir water flooding: For a type 1 reservoir sample (such as well 4372-2), the permeability of the Chang 8 layer is 1.47×10^{-3} μm^2, and the starting pressure is 0.039 MPa. When the injected water reaches 0.7PV, the model outlet has seen water, but the spread area is small. When the pressure is raised to 0.089 MPa, the area of permeability the injected water increases. For the two types of reservoir samples (such as well 4723-3), the permeability of the Chang 8 layer is $0.29\times10^{-3}\mu m^2$, and the starting pressure is 0.057MPa. When the injected water reaches 1PV, the model exits the water, and then the injected water stop flowing. When the pressure is raised to 0.102 MPa, the injected water reflows (Fig. 1). In the initial stage of displacement, the injected water first advances along the large pores. As the displacement pressure increases, the injected water continuously pushes into the small pores and forms a seepage channel. Since the oil droplets will have corresponding resistance during the displacement process, this will make it impossible to pass through the previously formed seepage channel. During the displacement process, it is also found that when some oil droplets passed through the small throat, the oil droplets were stuck, increasing the displacement pressure and still not moving. Taking 4354 as an example, when the displacement pressure reaches 0.79 MPa, the oil drop can not move at the throat. At this time, the displacement pressure is increased again, and when the

pressure was increased to 0.117 MPa, it is still unable to move. It can be seen from the analysis that the starting pressure of the better reservoir is lower than that of the poor reservoir and the water and oil flow was easy. The pore throat characteristics of tight sandstone reservoirs seriously affect water flooding efficiency. The small pore throat had a great influence on the seepage characteristics of the reservoir, which will reduce the oil displacement efficiency and also form a "crack" phenomenon. The seepage of smaller pore throat oil in the reservoir acts as a counteraction, which will prevent the movement of some oil droplets, and will “lock” the established flow channel that has formed in the initial stage of seepage to reduce the oil displacement efficiency.

3.2. Microscopic model water flooding experiment

It can be seen from Table 2 that the oil displacement efficiency of the 8th reservoir in the study area was 24.23%, the minimum was 9.00%, and the average was 18.37%.

Table 2. Microscopic model water flooding efficiency statistics

Hashtag	Layer	Number	Reservoir type	Permeability $\times10^{-3}\mu m^2$	1PV	2PV	3PV
					Ed/%		
4103-4	Chang 8	7	2	0.17	18.56	30.12	36.57
4123-1		2	3	0.081	13.33	22.50	23.54
4372-2		1	2	0.23	23.03	32.95	33.77
4107-2		5	3	0.092	9.00	17.00	20.78
4109-3		9	3	0.28	17.73	26.36	28.18
43032-3		3	1	2.57	20.86	33.26	43.25
4355-2		2	1	1.47	24.23	42.77	55.32
4354		5	2	0.41	20.56	32.22	36.67
4363		7	2	0.30	14.00	19.00	38.61
4723-3		8	2	0.34	13.51	27.02	31.28
Average				0.59	18.37	32.18	37.45

The maximum oil displacement efficiency at 2PV is 42.77%, the smallest. It was 17.00% with an average of 32.18%; the maximum oil displacement efficiency at 3PV is 55.32%, the minimum is 20.78%, and the average is 37.45%. The overall oil displacement efficiency is low, and the water drive is poor in Chengdu. The better the reservoir type, the higher the oil displacement efficiency, the poorer reservoir type and the relatively low oil displacement efficiency. The oil displacement efficiency of the first-class reservoir samples ranged from 43.25 to 55.32%, the oil displacement efficiency of the two types of reservoir samples ranged from 31.28 to 38.61%, and the three types of reservoir samples flooded between 20.78 and 28.18%. Factors such as poor physical properties, small pore throat and strong heterogeneity in the study area have seriously affected the water flooding efficiency of the reservoir. It is also found from the real sandstone micro-water flooding experiment that the strong heterogeneity of the reservoir pore-throat distribution causes the “circulation” phenomenon of the remaining oil, forming a residual oil of the continuous film. The difference in the characteristics of the pore throat was obvious, and it also caused a "crack" phenomenon.

3.3. Core water flooding nuclear magnetic resonance

The results of core water flooding nuclear magnetic resonance were summarized in Table 3. It can be seen from Table 3 that the storage properties of the first-class reservoir samples were well, the initial oil saturation was 55.02%, the physical properties of the two types of reservoir samples were general, the initial oil saturation was 57.11%, the physical properties of the three types of reservoir samples were poor, and the initial oil saturation was 39.57%, 1, 2 reservoirs had a higher percentage of movable oil,

and the third group of reservoirs had a lower percentage of movable oil. This indicates that the better reservoir initial oil saturation and the percentage of movable oil were also higher.

Table 3. Partial water flooding NMR test results

Hashtag	Layer	Number	Reservoir type	Porosity /%	Permeability $\times10^{-3}\mu m^2$	IOS /%	POM /%	MOS /%	DE /%
4372-2	Chang 8	6	3	7.33	0.074	39.57	55.49	21.41	32.65
4107-2		2	3	6.16	0.067	46.92	38.67	18.24	28.05
43032-3		4	2	11.49	0.69	57.11	50.97	28.77	36.45
4355-2		2	1	12.26	1.83	55.02	71.35	39.27	49.51
4354		1	2	10.31	0.53	53.31	51.69	27.56	35.40

Note: IOS-Initial oil saturation; POM- Percentage of movable oil; MOS-Movable oil saturation; DE-Displacement efficiency

4. Conclusion

The Chang 8 reservoirs are divided into three categories. The main parameters are porosity, permeability, median pressure, sorting coefficient, T2 cutoff value, pore throat radius, pore throat combination, pore type and diagenetic facies. Among them, the first type of reservoir is a good reservoir, the porosity is ≥12%, the permeability is $1\sim10\times10^{-3}\mu m^2$, the pore throat radius is ≤ 2μm, the median pressure is 3.5~8.5 MPa, and the sorting coefficient is between 2.34~2.47, T2 cutoff value ≥ 100ms, pore throat combination type is medium pore fine throat type, pore type is intergranular pore, dissolution pore and micro crack; type 2 reservoir is medium reservoir, porosity is 8~12 %, the permeability is $0.1\sim1\times10^{-3}\mu m^2$, the throat radius is 0.5~2μm, the median pressure is 8.5~17.6MPa, the sorting coefficient was between 2.47~2.56, and the T2 cutoff value is between 45~100ms. The throat type is small throat type, the pore type is intergranular pore and dissolution pore; the third type reservoir is poor reservoir, porosity ≤8%, permeability $\leq0.1\times10^{-3}\mu m^2$, pore throat radius ≤ 0.5μm, the median pressure is 17.6~28.1MPa, the sorting coefficient is between 2.56~2.67, the T2 cutoff value is ≤45ms, the pore throat combination type is fine pore throat type, and the pore type is intergranular pore. The percentage of movable oil in core samples of Class 1 and Class 2 reservoirs is higher than that of Class 3 reservoirs. The better the reservoir type, the higher the oil displacement efficiency, the poorer reservoir type and the relatively low oil displacement efficiency. The type 1 reservoir displacement type is mainly uniform displacement and reticular displacement type; the second type reservoir displacement type was mainly dendritic displacement type; the third type reservoir displacement type was mainly serpentine displacement type.

Acknowledgments

This work is financially supported by the grants from Scientific Research Program Funded by Shaanxi Provincial Education Department (18JS089) and National Science Foundation of China (21808182).

References

[1] C.Z. Jia, C. Zou, J.Z. Li, et al. Evaluation criteria, main types, basic characteristics and resource prospects of China's tight oils, Acta Petrolei Sinica, 33 (2012) 343-350.
[2] X.G. Tong, The genesis and distribution of unconventional oils, Acta Petrolei Sinica, 33 (2012) 20-26.
[3] C. Zou, G.S. Zhang, Z. Yang, et al. Concept, characteristics, potential and technology of unconventional oil and gas-concurrently on unconventional oil and gas geology, Petroleum Exploration and Development, 40 (2013) 385- 399.
[4] Z. Dong, S.A. Holditch, D.A. Mcvay, Global unconventional resource assessment, SPE Economics & Management, 4 (2012) 222-234.
[5] H. Yang, S.X. Li, X.Y. Liu, Characteristics and resource potential of tight oil and shale oil in

Ordos Basin, Acta Petrolei Sinica, 34 (2013) 1-11.
[6] C. Zou, Z. Yang, S.Z. Tao, et al. Nano-hydrocarbons and source-storage symbiotic oil and gas accumulation, Petroleum Exploration and Development, 39 (2012) 13-26.
[7] C. Zou, D.Z. Dong, S.J. Wang, et al. Formation mechanism geological characteristics and resource potential of shale gas in China, Petroleum Exploration and Development, 37 (2010) 641-653.
[8] C. Zou, R.K. Zhu, B. Bai, et al. The first discovery of nanopores in China's oil and gas reservoirs and its scientific value, Acta Petrologica Sinica, 27 (2011) 1857-1864.
[9] R.G. Loucks, R.M. Reed, S.C. Ruppel, Morphology, genesis, and distribution of nanometer-scale pores in siliceous mudstones of the Mississippian Barnett Shale, Journal of Sedimentary Research, 79 (2009) 848-861.
[10] Z.L. Wang, Research progress, existing problems and development trends of tight rock oil, Petroleum Experimental Geology, 35 (2013) 587-595.
[11] C.X. Wang, Q. Luo, Y. Song, et al. Discussion on nano-oil geology-unconventional oil and gas geology theory and research methods, Petroleum Geology & Experiment, , 36(2014) 659-667.
[12] H. Liang, X.N. Li, Qi. Ma, et al. Geological characteristics and exploration potential of tight oil in the strip lake group of Santanghu Basin, Petroleum Exploration and Development, 41 (2014) 563-572.
[13] L.Z. Shi, Z.Z. Wang, G. Zhang, et al. Formation conditions and distribution of tight oil in Qijia area, Songliao Basin, Petroleum Exploration and Development, 42 (2015) 1-7.
[14] Z.H. Zhai, K.G. Osadetz, Evaluation of tight oil resources in the Cardium group of sedimentary basins in Western Canada, Petroleum Exploration and Development, 40 (2013) 320-328.
[15] G. Chen, J. Lin, W.M. H., X.F. Gu, et al. Characteristics of a crude oil composition and its in situ waxing inhibition behavior, Fuel., 218 (2018) 213-217.